Evidence for the Chemical Activation of Essential Cys-302 upon Cofactor Binding to Nonphosphorylating Glyceraldehyde 3-Phosphate Dehydrogenase from *Streptococcus mutans*†

Stéphane Marchal and Guy Branlant*

Maturation des ARN et Enzymologie Moléculaire, UMR 7567 CNRS-UHP, Université Henri Poincaré Nancy I, Faculté des Sciences, B.P. 239, 54506 Vandoeuvre-Les-Nancy Cédex, France

Received February 25, 1999; Revised Manuscript Received June 14, 1999

ABSTRACT: Nonphosphorylating glyceraldehyde 3-phosphate dehydrogenase (GAPN) from *Streptococcus mutans* which catalyzes the irreversible oxidation of D-glyceraldehyde-3 phosphate (D-G3P) into 3-phosphoglycerate (3-PGA) in the presence of NADP belongs to the aldehyde dehydrogenase (ALDH) superfamily. Oxidation of D-G3P into 3-PGA by GAPN involves the formation of a covalent enzyme intermediate via the nucleophilic attack of the invariant Cys-302. Titration of Cys-302 in the apo-enzyme by two different kinetic probes, iodoacetamide and 2,2′-dipyridyl disulfide, shows a pK_{app} of 8.5 and a chemical reactivity surprisingly low compared to a reactive and accessible thiolate. Binding of NADP causes a strong increase of the reactivity of Cys-302—which is time dependent—with a pK_{app} shift from 8.5 to 6.1. Concomitant with the increase in the Cys-302 reactivity, an additional protein fluorescence quenching is observed. These data suggest that cofactor binding induces at least a local conformational rearrangement within the active site. The efficiency of the rearrangement depends on the structure of the cofactors and on the protonation of an amino acid with a pK_{app} of 5.7. The rate of the rearrangement also strongly increases when temperature decreases. The data on the conformational rearrangement also reveal an amino acid with a pK_{app} of 7.6 whose deprotonation increases the reactivity of the thiolate of Cys-302 by a 3-fold factor. The nature of the amino acid involved—which should be located close to Cys-302 in the holo-active form—is likely the invariant Glu-268. Changing Glu-268 into Ala or Cys-302 into Ala leads to mutants in which the rearrangement is only efficient in the presence of saturating concentrations of both NADP and G3P. The structural aspects of the conformational rearrangement occurring during the catalytic process in the wild-type GAPN should include at least reorientation of both Cys-302 and Glu-268 side chains and repositioning of the nicotinamide ring of the cofactor to permit the chemical activation of Cys-302 and the formation of an efficient ternary complex. Thus, it is likely that the conformation of the active site in the reported X-ray structures of ALDHs determined so far in the presence of cofactor, in which the side chains of Cys-302 and Glu-268 are 6.7 Å apart from each other, does not represent the biological active form.

Nonphosphorylating glyceraldehyde 3-phosphate dehydrogenase (GAPN)[1] from *Streptococcus mutans* is postulated to supply the lack of NADP reducing enzymes of the oxidative hexose phosphate pathway (*1*). It catalyzes the irreversible oxidation of D-glyceraldehyde 3-phosphate (D-G3P) into 3-phosphoglycerate (3-PGA) in the presence of cofactor NAD(P). It belongs to the aldehyde dehydrogenase (ALDH) superfamily which oxidizes a wide variety of aldehydes into acidic compounds (*2*, *3*). The oxidoreduction step of the catalytic mechanism consists of a hydride ion transfer occurring from the aldehydic carbon of the substrate to the C-4 position of the nicotinamide ring of the coenzyme. From a chemical point of view, the hydride transfer can only occur if the aldehydic group is first converted into a tetrahedral intermediate. Evidence derived from kinetics (*4*, *5*), affinity labeling (*6*, *7*), and directed mutagenesis (*8*) carried out on several ALDHs has demonstrated that a covalent intermediate is formed via the nucleophilic attack of the conserved Cys-302 (*9*). Therefore, the reaction pathway in G3P oxidation by GAPN involves two steps: first, the formation of a covalent ternary complex GAPN−NADP−G3P preceding the oxidoreduction that leads to a thioacyl intermediate and NADPH and, second, the deacylating step (see Figure 1). The fact that GAPN is highly active at neutral pH implies that Cys-302 must be in a thiolate form at physiological pH. Therefore, the active site environment of GAPN is such that it should decrease the Cys-302 pK_{app}, thereby increasing the nucleophilicity of Cys-302. Inspection of the environment of the essential Cys-302 of the four

† This research was supported by the Centre National de la Recherche Scientifique and the University Henri Poincaré Nancy I.

* To whom all correspondence should be sent. Phone: 33 3 83 91 20 97. Fax: 33 3 83 91 20 93. E-mail: guy.branlant@maem.uhp-nancy.fr.

[1] Abbreviations: ALDH, aldehyde dehydrogenase; GAPN, nonphosphorylating glyceraldehyde 3-phosphate dehydrogenase; GAPDH, phosphorylating glyceraldehyde 3-phosphate dehydrogenase; *S. mutans*, *Streptococcus mutans; E. coli*, *Escherichia coli;* D-G3P, D-glyceraldehyde 3-phosphate; 3-PGA, 3-phosphoglycerate; IAM, iodoacetamide; 2PDS, 2,2′-dipyridyl disulfide; DTNB, 5,5′-dithiobis(2-nitrobenzoate); TES, *N*-(tris(hydroxymethyl)methyl)-2-aminoethanesulfonic acid.

10.1021/bi990453k CCC: $18.00
Published on Web 09/03/1999

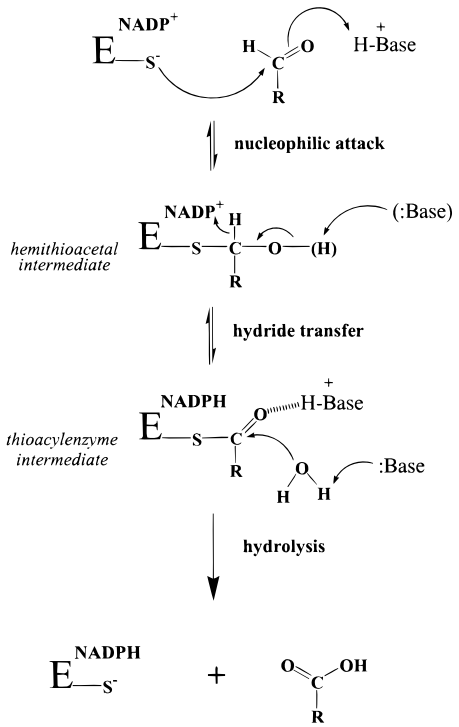

FIGURE 1: Schematic representation of the postulated catalytic mechanism of nonphosphorylating GAPDH. R represents the CH(OH)COOP part of the substrate D-G3P. A base is postulated to favor the hydride transfer from the thiohemiacetal intermediate toward the pyridinium ring. An alternative would be a protein environment like an oxyanion hole, sufficient to decrease the pK_a of the hydroxyl of the thiohemiacetal intermediate, permitting an efficient hydride transfer without base-catalyst assistance.

ALDH X-ray structures available so far (*10*−*13*) does not give clear indications on the nature of the structural factors which could be involved in decreasing pK_{app} of the Cys-302 thiol group. Except for the presence of the positive charge of the nicotinamide ring of cofactor and of the amide peptide nitrogens of residues 302 and 303, no structural elements such as side chains and N-terminus part of any α helix are located within a 5 Å sphere centered on the thiol group that can contribute to the stabilization of the thiolate.

In the present study, the pK_{app} value and chemical reactivity of Cys-302 have been determined in the absence and in the presence of saturating concentration of NADP in wild-type and E268A mutant GAPNs from *S. mutans*. The binding of NADP has been studied by following the quenching of Trp fluorescence. The results show that cofactor binding induces a conformational rearrangement[2] within the active site that leads to a high chemical reactivity of Cys-302 and a pK_{app} shift from 8.5 to 6.1. Additionaly, the deprotonation of the side chain of an amino acid with a pK_{app} of 7.6, whose nature is likely Glu-268, located close to Cys-302 in the active holo-form, also increases the reactivity of Cys-302. The conformational rearrangement is also shown to be more efficient at low temperature and to depend on the nature of the cofactor and on the protonation of an amino acid with a pK_{app} of 5.7. All the results are discussed in relation with the available three-dimensional structures of ALDHs.

[2] The conformational rearrangement can include as little as reorientation of the side chains of Cys-302 and Glu-268 and repositioning of the nicotinamide ring of the NADP or a more profound transition.

MATERIALS AND METHODS

Site-Directed Mutagenesis, Production, and Purification of Wild-Type and Mutant Enzymes. The *Escherichia coli* strain used for production of wild-type and mutant GAPNs was DH 5α (supE44, lacU169 (80 lacZM15), hsdR17, recA1, endA1, gyrA96, thi-1, relA1) transformed with a plasmidic construction containing the *gapN* gene (*14*) under the control of the lac promoter. Site-directed mutagenesis was performed using the method of Kunkel et al. (*15*).

The purification procedure was carried out as previously described (*1*), except that the gel filtration step was replaced by a phenyl-Sepharose column. All the enzymes were isolated as apo form as judged by the absorbance ratio 280/260 of 2 and by the fact that no released cofactor was enzymatically detectable after acidic denaturation.

Enzyme purity was checked by electrophoresis on 7.5% SDS−PAGE (*16*). The subunit molecular weights of wild-type and mutant GAPNs were verified by mass spectrometry. The relative molecular mass of native wild-type GAPN was estimated by gel-filtration chromatography on a Superose 12 HR column in buffer A. Thyroglobulin (670 kDa), bovine globulin (158 kDa), chicken ovalbumin (44 kDa), horse myoglobin (17.5 kDa), and B12 vitamin (1.35 kDa) were used as references. GAPN concentration was estimated spectrophotometrically, using an extinction coefficient of 2.04 × 10^5 M^{-1}·cm^{-1}, as deduced from the method of Scopes (*17*).

Enzyme Kinetics and Dissociation Constant K_D Determination. Initial rate measurements were carried out at 25 °C on a Kontron Uvikon 933 spectrophotometer by following the appearance of NADPH at 340 nm. The standard experimental conditions were 1 mM NADP, 0.2 mM G3P, 50 mM TES buffer, and 5 mM β-mercaptoethanol, pH 8.2. Catalytic constants k_{cat} and K_M were determined by measuring steady-state velocity at various D-G3P and NAD(P) concentrations, and data were plotted according to an ordered bisubstrate mechanism with competitive substrate inhibition (*18*).

NAD(P) binding was followed by tryptophan fluorescence quenching on a SAFAS flx spectrofluorometer at 25 °C. Fluorescence measurements were carried out in 50 mM phosphate buffer at pH 6.0 and 8.5. The excitation wavelength was set at 297 nm, and spectra were recorded in the range 320−400 nm. Maximum emission intensity was observed at 334 nm. NAD(P) binding affinities were determined as previously described (*19*). NAD(P)H bindings were determined by measuring the fluorescence emission of reduced cofactors in the presence and the absence of enzyme. The data were analyzed by the Koltz equation as developed by Stockell (*20*):

$$\frac{d}{p} = \frac{K_D}{e - p} + n$$

Here d is the total concentration of ligand, e is the enzyme concentration, p is the fraction of enzymatic sites bound multiplied by e, K_D is the dissociation constant, and n is the number of binding sites. Plots of d/p versus $1/(e - p)$ are linear provided that the binding sites are equivalent and independent. The slope corresponds to K_D value while the ordinate intercept is n.

Cysteine Content in Wild-Type Enzyme Measured with 5,5′-Dithiobis(2-Nitrobenzoate) (DTNB) and 2,2′-Dipyridyl Disulfide (2PDS). The amount of cysteines was deduced from the absorbance of thionitrobenzoate and pyridine-2-thione using extinction coefficients of 13 600 M^{-1} cm^{-1} at 412 nm and 8080 M^{-1} cm^{-1} at 343 nm, respectively. The enzyme was dissolved in 50 mM phosphate buffer pH 8.2, and the sulfhydryl reagent was added in a large excess relative to the enzyme. SDS (1% final) was also added for measurements under denaturing conditions.

Kinetic Reactions with 2PDS. Due to the high reactivity of Cys-302 in the holo wild-type enzyme and of the glutathione cysteine, fast kinetic measurements were carried out on a Biologic Instrument (SFM3) stopped-flow apparatus. Glutathione kinetic reaction with 2PDS was carried at 25 °C under pseudo-first-order conditions in 30 mM acetic acid, 30 mM imidazole, 120 mM Tris/HCl buffer at constant ionic strength of 0.15 M over a pH range of 5 to 9.8 (buffer B). The second-order rate constants k_2 were determined at each pH and then fitted to the eq 1, in which k' represents the

$$k_2 = k'\left(\frac{1}{10^{(pK_{app}-pH)}+1}\right) \quad (1)$$

second rate constant for the thiolate form.

In the case of holo wild-type enzyme, Cys-302 reaction with 2PDS was so rapid that it occurred in the dead time of the stopped-flow apparatus. Kinetics with 2PDS were only performed at pH 9 in buffer B. Under the experimental conditions used, the concentration of NADP was maintained at 25-fold excess relative to the enzyme.

When cysteine reactivities were low, rate measurements were carried on a Kontron Uvikon 933 spectrophotometer. Second-order rate constants were determined for Cys-382 in holo wild-type, apo-like[3] E268A mutant and C302A mutant enzymes but only at pH 9. Similarly, second-order rate constants were determined for Cys-302 in apo-like E268A mutant and C302A mutant enzymes. pH-dependences of the 2PDS reactions with apo wild-type and mutant GAPNs were performed at 25 °C in buffer B over a pH range 5−9.8 under pseudo-first-order conditions. At pH higher than 9.8, the enzyme was not stable. The pseudo-first-order k_{obs} were determined at each pH fitting the absorbance A at 343 nm versus time t to eq 2, where a_1 is the burst magnitude, $k = k_{obs}$, and c represents the value of the ordinate intercept.

$$A = a_1(1 - e^{-kt}) + c \quad (2)$$

The second-order kinetic constants k_2 were calculated dividing k_{obs} by the concentration of 2PDS and were fitted to the eq 1.

pH-Dependence of the Alkylation Reactions with Iodoacetamide (IAM). Alkylation rates for wild-type and mutant GAPNs were determined over a pH range 5−9.8 in buffer B at 25 °C. In the case of the holo wild-type and the apo-like form of E268A mutant, NADP concentration was fixed largely above its K_D value. The pseudo-first-order k_{obs} were determined at each pH from plots of $\ln(A_0/A)$ versus time (A_0 is the initial enzymatic activity and A is the activity at time t). The standard deviation on each individual k_{obs} values was below 5%, based on at least three independent determinations. The second-order kinetic constants k_2 were calculated dividing k_{obs} by the concentration of IAM at each pH and were then fitted to eq 1 or to eq 3 to determine the best-fit pK_{app}'s, in which k' and k'' represent two different second-order rate constants for the thiolate form.

$$k_2 = k'\left(\frac{1}{10^{(pK_{app1}-pH)}+1}\right)\left(\frac{1}{10^{(pH-pK_{app2})}+1}\right) + k''\left(\frac{1}{10^{(pK_{app2}-pH)}+1}\right) \quad (3)$$

Study of the Factors Affecting the Efficiency of the Conformational Rearrangement. (a) *pH and Cofactors*. Apo wild-type GAPN was dialyzed at 4 °C against 50 mM phosphate buffer at various pH values (5−8.2) and was then saturated by an excess of NADP, NADPH, or NADH with respect to the enzyme concentration. The samples were then incubated at 4 °C. Aliquots were withdrawn at different time intervals, and the fast reacting DTNB accessible Cys-302 was measured as the initial A at 412 nm at 25 °C in 50 mM phosphate buffer, pH 8.2. The pseudo-first-order k_{obs} were determined at each pH, fitting the values corresponding to the instantaneous absorbance at 412 nm versus time t to eq 2. For each cofactor, the data were fitted to eq 4 to determine pK_{app}, where k_{max} and k_{min} represent the maximal and minimal k_{obs} values and b is the slope parameter.

$$k = \frac{k_{max}}{1 + e^{b(pH-pK_{app})}} + k_{min} \quad (4)$$

(b) Temperature. Apo wild-type GAPN was dialyzed against 50 mM phosphate buffer at pH 5.5. Two types of experiments were done, namely in the absence and the presence of 30% glycerol permitting in the latter case to test temperature lower than 0 °C. In both cases, the enzyme was saturated by an excess of NADPH and the fast reacting DTNB accessible Cys-302 was measured. The pseudo-first-order constants k_{obs} were determined for each temperature, fitting the values corresponding to the instantaneous appearance of absorbance at 412 nm versus time to eq 2.

Kinetic Studies of Fluorescence Quenching. Fluorescence emission spectra were recorded on a SAFAS flx spectrofluorometer equipped with a thermostated cell. After excitation at 297 nm, quenching of tryptophan fluorescence was recorded in the 320−400 nm range and was corrected from the Raman contribution. The maximum of emission was observed at 330 mn.

Apo wild-type and E268A and C302A mutant GAPNs were dialyzed against 50 mM phosphate buffer, pH 5.5. To each sample of enzyme maintained at 4 °C, an excess of NADP was added. Periodically, aliquots were withdrawn and the fluorescence emission spectrum was then recorded for each sample. In parallel, the intrinsic fluorescence was measured for each apo-enzyme.

The maximal emission values obtained for the wild type were plotted versus time and fitted to the eq 5, where $F_N(t)$ is the maximal fluorescence intensity at 330 nm, a_1 is the

[3] The term "apo-like form" indicates an apo-form enzyme saturated by cofactor but in which the cofactor has not yet induced the local conformational rearrangement.

burst magnitude, k is the apparent rate constant, and c represents the fluorescence of the ordinate intercept.

$$F_N(t) = a_1 e^{-kt} + c \quad (5)$$

RESULTS

Biochemical Properties of Wild-Type GAPN. GapN-encoded protein was overexpressed in *E. coli* strain. Over 30% of the soluble proteins in the supernatant were GAPN. The subunit molecular mass of 51 100 Da determined by mass spectrometry was in good agreement with the 51 090 Da mass predicted from the *gapN* DNA sequence. The elution profile of GAPN on gel filtration superose column under native conditions was in agreement with a tetrameric state (profile not shown).

Thiol reagents revealed two reactive cysteines per monomer under denaturing conditions. This result was expected from the *gapN* DNA sequence that indicates two cysteine residues at positions 302 and 382 (*14*). Under native conditions, Cys-302 and Cys-382 were also reactive in apo GAPN, showing similar but slower kinetics (see reaction with 2PDS, below). This indicated that, in addition to essential Cys-302 that is expected to be reactive, Cys-382 is also reactive in the apo structure. Inspection of the X-ray structure of bovine mitochondrial ALDH (*10*) shows that position 382 is located on the surface of the quaternary structure and thus is likely accessible to thiol reagents (stereoview not shown).

Enzymatic and Binding Properties of Wild-Type and Mutant GAPNs. K_M and k_{cat} values of wild-type GAPN were 24.5 μM and 67 s^{-1} for NADP and 6000 μM and 15 s^{-1} for NAD, respectively, with a K_M value of 50 μM for D-G3P. Mutation of Cys-382 did not significantly change the kinetic parameters, while substituting Ala for invariant Cys-302 abolished all activity. GAPN showed optimum velocity at pH 8.2, which was decreased by a factor of 2 at pH 7.2 (curve not shown). Changing the invariant Glu-268 into Ala did not significantly change the K_M values of the (co)substrates but led to a drastic decrease in k_{cat} by a 750-fold factor, as already described *(21, 22)*.

K_D values of wild-type GAPN for oxidized and reduced cofactors were determined at 25 °C by following the quenching of protein tryptophan fluorescence and the reduced coenzyme fluorescence increase upon coenzyme binding, respectively (curves not shown). Under our experimental conditions, the binding of cofactors was stoichiometric with one cofactor molecule per subunit. K_D values of 2.3, 517, 0.3, and 6 μM for NADP, NAD, NADPH, and NADH, respectively, were found at both pH 6.0 and pH 8.5. Moreover, values similar to 2.3 μM were determined for the NADP dissociation constant for the wild-type and mutant enzymes at pH 6.0 and at pH 8.5 (curves not shown).

Kinetics of the Reaction of Apo Wild-Type and Mutant GAPNs with 2PDS and IAM. The reaction of 2PDS with apo wild-type GAPN obeyed pseudo-first-order kinetics with formation of 2 mol of pyridine-2-thione per subunit, as determined from the absorbance change at 343 nm. The pH−k_2 curve fitted better to a monosigmoidal profile with a pK_{app} value of 8.84 and a k' value of 1350 $M^{-1}\cdot s^{-1}$ than to a double sigmoidal profile with pK_{app} values of 8.54 and 8.83 and k' values of 517 and 864 $M^{-1}\cdot s^{-1}$ for Cys-302 and Cys-382, respectively (see comment in legend of Figure 2). C382A mutant behaved similarly to wild-type enzyme except that only 1 mol of 2PDS reacted/subunit. A pK_{app} value of 8.49 for Cys-302 and a k' value of 225 $M^{-1}\cdot s^{-1}$ were determined from the pH−k_2 curve. A pK_{app} value of 9.07 for Cys-382 and a k' value of 588 $M^{-1}\cdot s^{-1}$ were determined from similar studies done on the C302A mutant. Thus, the pK_{app} of 8.84 determined in the wild-type GAPN represented the contribution of both Cys-302 and Cys-382 with pK_{app} of 8.5 and 9.1, respectively. E268A mutant showed a behavior which is similar to the wild type with a pK_{app} of 8.81 and a k' value of 475 $M^{-1}\cdot s^{-1}$. The C382A/E268A double mutant exhibited a behavior comparable to C382A mutant with a pK_{app} of 8.50 for Cys-302 and a k' value of 500 $M^{-1}\cdot s^{-1}$ (see Table 1, curve not shown).

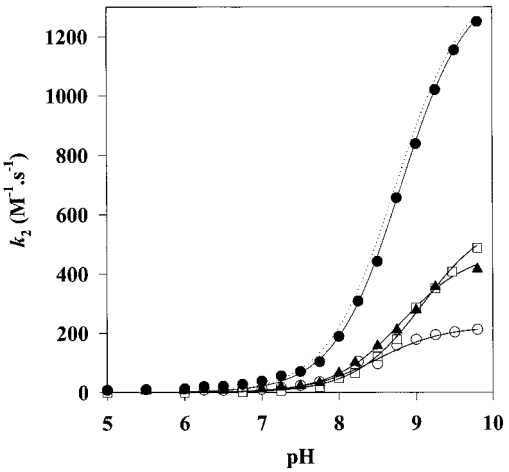

FIGURE 2: pH-dependence of the second-order rate constant k_2 for the reaction of the thiol group with 2PDS of wild-type (●), C382A mutant (○), E268A mutant (▲), and C302A mutant (□) apo-enzymes. Reaction kinetics were performed at 25 °C over a pH range of 5−9.8 in buffer B. The concentration of enzymes were 3.71 μN (in sites) and 2PDS concentration was 111 μM. Values of k_{obs} were determined using nonlinear regression analysis, and second-order rate constants k_2 were fitted to eq 1 (see also Materials and Methods). Wild-type data were best fitted against a one-pK_a model (solid line theorical curve, pK_{app} of 8.84), which gave a residual sum of square of 2116 than against a two-pK_a model (dotted line theoretical curve, pK_{app}'s of 8.54 and 8.83) which yielded a residual sum of square of 1923.

IAM inactivation of apo wild-type enzyme and C382A, E268A, and C382A/E268A mutants also followed pseudo-first-order kinetics. Kinetic data with different initial enzyme concentrations confirmed the first-order dependence on enzyme concentration for each enzyme (curves not shown). The pH−rate profiles showed a sigmoidal behavior with a pK_{app} of 8.39, 8.49, 8.45, and 8.49 and k' constants of 10.2, 5.17, 4.40, and 5.17 $M^{-1}\cdot s^{-1}$ for wild-type GAPN and C382A, E268A, and C382A/E268A mutants, respectively (see Figure 3 B and Table 1).

Kinetics of the Reaction of Holo Wild-Type GAPN with 2PDS, DTNB, and IAM. Holo wild-type enzyme was obtained by incubation of the apo-enzyme for 4 h at 4 °C and pH 5.5 in the presence of saturating concentration of NADP or NADPH (see next paragraphs). Two cysteines were reactive with 2PDS and DTNB. One cysteine reacted very rapidly in the dead time of a stopped-flow apparatus with a 30-fold excess of 2PDS or 40-fold excess of DTNB with respect to the enzyme site concentration. The same behavior was also observed in the presence of a 10-fold excess of 2PDS or DTNB. A similar result was obtained on C382A mutant. Altogether, these results indicated that, under the

Table 1: Second-Order Rate Constants for the Reaction of the Thiol Group with 2PDS and IAM for the Wild-Type and Mutant Apo-Enzymes

	reactive cysteine	k'_{Cys},[c] $M^{-1}\cdot s^{-1}$	pK_{app} of Cys
	Apo-Form GAPN		
wild type			
+2PDS	Cys-302, Cys-382	1350 ± 28	8.84 ± 0.04
+IAM	Cys-302	10.2 ± 0.2	8.39 ± 0.10
C382A mutant			
+2PDS	Cys-302	225 ± 9	8.49 ± 0.07
+IAM	Cys-302	5.17 ± 0.08	8.49 ± 0.02
C302A mutant			
+2PDS	Cys-382	588 ± 14	9.07 ± 0.02
E268A mutant			
+2PDS	Cys-302, Cys-382	475 ± 31	8.81 ± 0.08
+IAM	Cys-302	4.40 ± 0.05	8.45 ± 0.05
C382A/E268A mutant			
+2PDS	Cys-302	500 ± 17	8.50 ± 0.05
+IAM	Cys-302	5.17 ± 0.08	8.49 ± 0.07
	Phosphorylating GAPDH of *E. coli* (Apo-Enzyme)[b]		
+2PDS	Cys-149	(3.15 ± 0.07) × 10^5	5.56 ± 0.57
+IAM	Cys-149	234 ± 3	5.75 ± 0.29
	Glutathione		
+2PDS		(5.34 ± 0.09) × 10^4	8.88 ± 0.02

[a] Kinetics of the reaction with 2PDS and IAM were determined over a pH range 5−9.8 at 25 °C. The experimental conditions are described in Materials and Methods. The second-order rate constants at each pH were fitted to a monosigmoidal equation to determine the pK_a's in Sigmaplot. The errors estimates are those provided by the program. [b] Data from ref *23*. [c] k'_{Cys} values corresponded to k' from eq 1.

Table 2: Second-Order Rate Constants for the Reaction of the Thiol Group with 2PDS and IAM for the Holo-Wild Type and for the Apo-like Mutants

	reactive cysteine	$k'_{Cys-302}$, $M^{-1}.s^{-1}$	pK_{app} of Cys	pK_{app} of "Y"[c]	$k''_{Cys-302,}$ $M^{-1}\cdot s^{-1}$	k_2 at pH 9, $M^{-1}\cdot s^{-1}$
			Holo-Form[e]			
wild-type GAPN						
+2PDS	Cys-302[b]	ND	ND	ND		> 2 × 10^5
	Cys-382[b]	ND	ND	ND		13.0 ± 0.2
+IAM	Cys-302	57.0 ± 7.7[d]	6.10 ± 0.20	7.60 ± 0.10	182 ± 2[d]	
			Holo-Form with NADPH[f]			
wild-type GAPN						
+IAM	Cys-302	64 ± 9	6.78 ± 0.10	7.53 ± 0.13	164 ± 10	
			Apo-Like Form GAPN			
E268A mutant						
+2PDS	Cys-302[b]	ND	ND	ND		24 ± 1
	Cys-382[b]	ND	ND	ND		650 ± 18
+IAM	Cys-302	0.056 ± 0.001	8.47 ± 0.03			
C302A mutant						
+2PDS	Cys-382[b]	ND	ND	ND		600 ± 20
C382A mutant						
+2PDS	Cys-302[b]	ND	ND	ND		20.0 ± 0.5

[a] Kinetics of the reaction with 2PDS and IAM were determined over a pH range 5−9.8 at 25 °C. The experimental conditions are described in Materials and Methods. The second-order rate constants determined at each pH were fitted either to the monosigmoidal eq 1 or to the bisigmoidal eq 3 to determine the best-fit pK_a's. ND: not determined. [b] Reaction kinetics with 2PDS were only measured at pH 9. [c] The pK_{app} "Y" is the pK_{app} value of the residue that increases the reactivity of Cys-302. [d] The values of 57 and 182 $M^{-1}\cdot s^{-1}$ were calculated from eq 3 and correspond to k' and k'', respectively. [e] Holo-form refers to GAPN−NADP unless otherwise stated. [f] Conditions are equivalent to experiments for wild-type holoenzyme with NADP (Figure 3 legend).

stopped-flow experimental conditions used, Cys-302 was very reactive with a k_2 constant which can be estimated higher than 2 × 10^5 $M^{-1}\cdot s^{-1}$ at pH 9. Another cysteine, corresponding to Cys-382, was also reactive but with a k_2 constant of 13 $M^{-1}\cdot s^{-1}$ (determined with 2PDS as thiol reagent; see Table 2)—a 45-fold lower value than the one determined for Cys-382 in the apo C302A mutant (see Table 1).

The pH−rate profile for IAM alkylation of Cys-302 showed a double sigmoidal behavior with two pK_{app} of 6.1 and 7.6 and with k' and k'' values of 57 and 182 $M^{-1}\cdot s^{-1}$, respectively (see Figure 3A and Table 2).

Similar studies were carried out in the presence of saturating concentration of NADPH. The pH−rate profile showed a double sigmoidal behavior with two pK_{app} of 6.78 and 7.53 and with k' and k'' values of 64 and 164 $M^{-1}\cdot s^{-1}$, respectively (see Table 2).

Kinetics of the Reaction of Apo-like E268A Mutant with IAM and of Apo-like E268A, C382A/E268A, and C302A Mutants with 2PDS. All apo-forms of the mutants were incubated in the presence of saturating concentration of NADP at 4 °C for 18 h at pH 6.4 or for 5 h at pH 5.5 under conditions where the conformational rearrangement occurred in the wild-type enzyme.

The pH−rate profile for the IAM alkylation of Cys-302 in E268A mutant was of monosigmoidal form with a pK_{app} of 8.47 and a k' value of 0.056 $M^{-1}\cdot s^{-1}$ (see Table 2).

Two cysteines were reactive by 2PDS in E268A mutant with k_2 constants of 650 and 24 $M^{-1}\cdot s^{-1}$ at pH 9. Values of

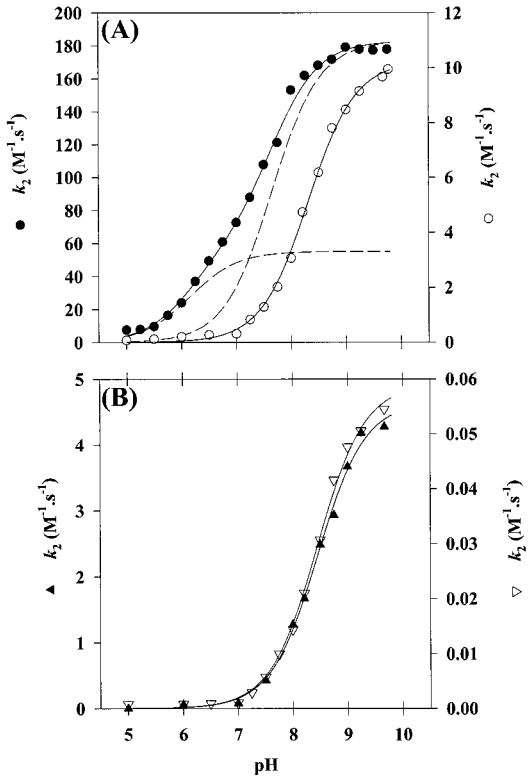

FIGURE 3: pH-dependence of the second-order rate constant k_2 for the reaction of Cys-302 with IAM of (A) apo (○) and holo (●) wild type and (B) apo E268 (▲) and apo-like E268A (▽) mutant. Alkylations rates were determined over a pH range of 5−9.8 at 25 °C in buffer B (see also Materials and Methods). Inactivation was carried out in test tube containing wild-type apoenzyme (20−1 μN) or holoenzyme (4−0.5 μN) with a 50- or 1000-fold excess of IAM with respect to the concentration of the essential −SH group, respectively. For apo and apo-like E268A mutant saturated by an 25-fold excess of NADP, enzymes (200−20 μN) were incubated with 1000-fold excess of IAM with respect to the concentration of the essential −SH group. Aliquots were withdrawn periodically, and residual activities were determined at 25 °C in 50 mM TES buffer pH 8.2 containing 5 mM β-mercaptoethanol. Second-order kinetic constants k_2 were calculated dividing pseudo-first-order constant k_{obs} by the concentration of IAM and were fitted to a monosigmoidal equation except for holo-wild type which was fitted to a bisigmoidal equation. For the holo-wild type, the broken lines correspond to contributions to k of each protonic state provided by the individual term of eq 3. The first pK_{app} of 6.1 corresponds to that of Cys-302, and the second one of 7.6 corresponds to that of a residue whose deprotonation increases the reactivity of Cys-302.

600 and 20 $M^{-1}\cdot s^{-1}$ for k_2 constants were determined on the C302A and C382A mutants, respectively. This suggested that the k_2 value of 650 $M^{-1}\cdot s^{-1}$ corresponded to the reactivity of Cys-382, which appears similar to the apo C302A mutant (see Table 2), while the k_2 value of 24 $M^{-1}\cdot s^{-1}$ corresponded to the reactivity of Cys-302.

Study of the Factors Influencing the Efficiency of the Conformational Rearrangement in the Wild Type. The efficiency of the conformational rearrangement was studied as a function of pH, of temperature, and of the nature of the cofactor. To evaluate quantitatively the effects of these factors, Cys-302 was used as a conformational probe. As already shown, Cys-302 chemical reactivity toward DTNB or 2PDS is at least 10^3-fold higher in the holo-form than in the apo-form. Taking in account the K_D values for NADP, NADPH, and NADH and the respective concentrations of apoenzyme and cofactors used, the fraction of the enzyme

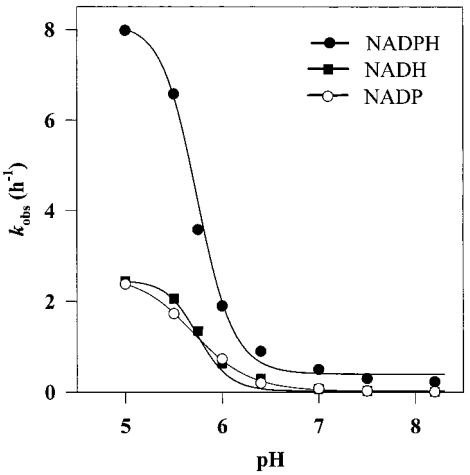

FIGURE 4: Effect of the pH on the rate of the apo → holo transition. Apo-wild type (200 μN in sites) was incubated at 4 °C in the presence of 5 mM NADP, 5 mM NADPH, or 50 mM NADH. At fixed time intervals, fast reacting Cys-302 was measured with DTNB at 25 °C in 50 mM phosphate buffer pH 8.2 with 7.35 μN enzyme sites and 300 μM DTNB. At each pH, k_{obs} values were calculated fitting the initial absorbance at 412 nm versus time to a single-exponential equation. For each cofactor, NADPH (●), NADH (■), and NADP (○), the pH−k_{obs} data were fitted with a monosigmoidal equation (see also Materials and Methods).

under the apo-conformation was in fact an enzyme with bound cofactor but in which cofactor had not induced the conformational rearrangement. In this apo-like form, the chemical reactivity of Cys-302 was at least 50-fold decreased compared to the apo-form (data not shown). Thus, the reactivity of Cys-302 measured at pH 9 is at least 10^4-fold higher in the holo-form than in the apo-like form and is at least 10^4-fold higher than that of Cys-382 (see also Tables 1 and 2). Thus, the extent to which the apo-like form progressed toward the holo-form in the incubation mixture was easily quantified by transferring an aliquot of this mixture at various time points to the DTNB reaction mixture and recording the initial absorbance at 412 nm. Under these experimental conditions, the cofactor concentrations in the cuvette remained largely higher than their K_D values. The pseudo-first-order k_{obs} values were determined from plots of these absorbances versus time using nonlinear regression analysis. Regardless of the experimental conditions studied, all the data fitted single-exponential rates well.

(a) Effect of the pH. This study was carried out at 4 °C with cofactors that only give an efficient conformational rearrangement. For each pH, varying from 5 to 8.2, a k_{obs} value was determined. As shown in Figure 4, pH−k_{obs} curves were of sigmoidal form with an activation process more efficient at acidic pH. A pK_{app} value of ∼5.7 can be determined with NADPH, NADH, and NADP. The fact that a similar pK_{app} was determined with NADH and NADPH indicated that the pK_{app} of 5.7 does not correspond to 2′-phosphate of the adenosine ribose but to the side chain of an amino acid whose protonation strongly accelerates the conformational rearrangement.

(b) Effect of the Nature of the Cofactor. These studies were done in the absence of glycerol, at 4 °C and at pH 5.5, under experimental conditions where a change in the rate of the conformational rearrangement was easily quantified for NADP, NADPH, and NADH and where the reduced cofactors remained chemically stable. As shown in Figure 4, the

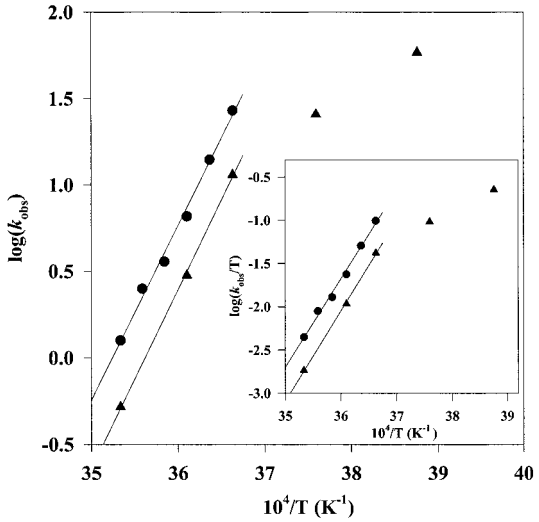

FIGURE 5: Effect of the temperature on the rate of the apo → holo transition**.** Apo-wild type was incubated in a 50 mM phosphate buffer at pH 5.5 in the absence (●) or presence of 30% glycerol (▲) at different temperatures. A 250-fold excess of NADPH was added with respect to the enzyme concentration (in sites). At fixed time intervals (0−2 h), fast reacting Cys-302 was measured with DTNB in 50 mM phosphate buffer, pH 8.2, at 25 °C with 7.35 μN enzyme sites and 300 μM DTNB. At each temperature, k_{obs} values were determined fitting the initial absorbance at 412 nm versus time to a single-exponential equation.

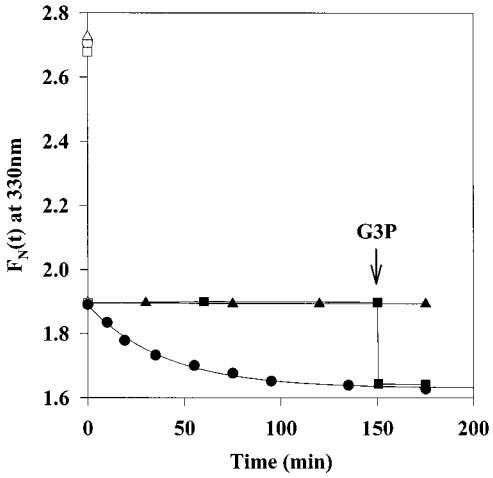

FIGURE 6: Time course of the GapN fluorescence change induced by NADP binding. After addition of 5 μM NADP, enzyme solutions at a final concentration of 200 μN were incubated at 4 °C, pH 5.5. At fixed time intervals, enzyme was withdrawn and dissolved in 50 mM phosphate buffer, pH 8.2, and fluorescence quenching was recorded for the wild type (●) and E268A (▲) and C302A (■) mutants (1 μN final) at 4 °C. Excitation and emission wavelengths were set at 297 and 330 nm, respectively. As a reference, intrinsic fluorescence was measured for the wild-type (○) and E268A (△) and C302A (□) mutant apo-enzymes (1 μN final) in the same conditions. For C302A mutant, 1 mM G3P was added (arrow) in the assay mixture after 150 min incubation of the apo-form in the presence of NADP at 4 °C.

rate of the rearrangement was higher for reduced cofactors but with a preference for NADP series.

(c) Effect of the Temperature. This study was done at pH 5.5 and in the presence of NADPH, which had been shown to be the most efficient coenzyme for the conformational rearrangement. Two types of experiments were carried out, in the absence and in the presence of 30% glycerol. As shown in Figure 5, plots of log k_{obs} and log k_{obs}/T as a function of $1/T$ are linear in the range 10−0 °C. Values of −193 and −196 kJ·mol^{-1} can be determined from the slopes of the curves, which can be ascribed to $E_a^{\ddagger}$ and $\Delta H^{\ddagger}$ differences between the apo-like form and the holo-form. The extrapolation of the line to infinite temperature gives a $\Delta S^{\ddagger}$ value of −0.86 kJ·mol^{-1}·K^{-1}. Similar values were obtained with NADP (data and curves not shown). The nonlinearity observed at temperature lower than 0 °C is likely due to an increase of the viscosity of the medium due to the presence of 30% glycerol.

Fluorescence Quenching of GAPN Used as a Tool To Follow the Conformational Rearrangement. Another means to follow the conformational rearrangement is to measure the quenching of the tryptophan fluorescence intensity upon coenzyme binding. GapN contains three tryptophan residues located either in the coenzyme-binding domain (Trp-13, Trp-56) or in the catalytic domain (Trp-375) (the location of these residues was deduced from the inspection of the X-ray structure of bovine mitochondrial ALDH). When wild-type and E268A and C302A mutant apo-enzymes were excited at 297 nm, a fluorescence emission maximum was observed at 330 nm. Incubating apo-wild type with NADP at saturating concentration under experimental conditions where conformational rearrangement has occurred led to a fluorescence quenching. This quenching is in fact the consequence of two additive effects: first, of the instantaneous binding of NADP to the apo-structure, which leads to 75% of the quenching, and second, of the conformational rearrangement, which is a function of time and which represents 25% of the quenching (see Figure 6). A k_{obs} value of 1.7 h^{-1} was determined for the conformational rearrangement step at pH 5.5 and at 4 °C, which is similar to that determined from Cys-302 reaction kinetics. The two mutants also exhibited a fluorescence quenching upon NADP binding at saturating concentration but which remained constant over time and represented 75% of the total fluorescence quenching observed for the holo-wild type. When a large excess of G3P was added to the inactive C302A mutant saturated by NADP, an instantaneous additional quenching of similar amplitude relative to the holo-form of the wild type was observed (see Figure 6).

DISCUSSION

Oxidation of D-G3P into 3-PGA by GAPN involves the formation of a covalent enzyme intermediate via Cys-302. Although activity is optimum at pH 8.2, it is about half at pH 7.2. Surprisingly, a pK_{app} of 8.5 was found for Cys-302 in the apo-enzyme with IAM and 2PDS probes, with a chemical reactivity much lower compared to a reactive and an accessible thiolate.

Binding of NADP caused a strong increase in the reactivity of Cys-302 with a pK_{app} shift from 8.5 to 6.1. Therefore, cofactor binding is able to induce, at least, a reorientation of the side chain of Cys-302 that renders Cys-302 more accessible and more reactive, at neutral pH. The additional fluorescence quenching observed after the formation of the apo-like structure whose rate is similar to that observed from Cys-302 modification also indicated that, concomitant with the increase in the Cys-302 reactivity, the environment of the quenched Trp changed. This could be due to a repositioning of either the cofactor or the quenched Trp or both.

The rate of the rearrangement depends on various factors, namely pH, temperature, the structure of the cofactors, and the protonation of an amino acid with a pK_{app} of 5.7. It is more efficient with NADP(H) than with NAD(H). This confirms the preference of GAPN for NADP cofactor (*14*). Regarding temperature effect, the results establish an unusual pattern of temperature behavior. The fact that plots of log k_{obs} and log k_{obs}/T as a function of $1/T$ are linear suggests that the reverse temperature variation of the rate of conformational rearrangement is the consequence of an entropic effect going from a random to a more ordered conformation of the apo-like form. This behavior can be interpretated in the light of recent structural studies of different ALDHs. As pointed out by Moore et al. (*13*), NAD^+ binding appears to be flexible and variable for the nicotinamide part of the cofactor in the ALDH enzymes. An explanation of our results is that temperature decrease would favor this entropically controlled transition by a minimization of thermal fluctuations. The enzyme would exploit this loss of entropy to modulate the active site geometry, mainly between Cys-302, Glu-268, and the nicotinamide ring, as such a better positioning of cofactor occurs. The fact that no lag phase was observed in the turnover kinetics between pH 5 and 9 on the time scale of a stopped-flow apparatus indicated that the binding of G3P to the binary complex enzyme−NADP, even under an apo-like conformation, led to the formation of an efficient ternary complex that considerably increased the rate of the conformational rearrangement.

The rearrangement induced by the cofactor binding also revealed an amino acid with a pK_{app} of 7.6 whose deprotonation increases the reactivity of the Cys-302 thiolate by a factor of 3. Thus, the rearrangement not only renders the Cys-302 more accessible and reactive but also brings the thiol group close to the side chain of an amino acid with a pK_{app} of 7.6. A likely candidate was the invariant Glu-268 whose mutation leads to a drastic k_{cat} decrease. Reaction of Cys-302 in the E268A mutant, in the presence of saturating concentration of NADP, gave a pK_{app} of 8.5 and a k_2 value similar to those determined for the apo wild-type enzyme. Therefore, these data indicated that, in the absence of Glu-268, NADP binding did not induce the rearrangement on the scale of time used, in contrast to what was observed for the wild-type enzyme. This was also confirmed by fluorescence quenching experiments which showed a quenching magnitude similar to that of the apo-like form but lower than that observed for the holo-form of the wild-type. This raised the question whether the absence of Glu-268 prevented the formation of an efficient catalytic turnover ternary complex. Indeed, the 750-fold decrease in k_{cat} could be the consequence of the absence of the conformational rearrangement in the mutant during the catalytic turnover. In fact, stopped-flow experiments carried out on the E268A mutant at pH 6 showed an acylation step with a rate of 60 s^{-1} similar to the wild type (Marchal, unpublished results), therefore indicating that G3P binding to the binary complex E268A mutant−NADP apo-like structure leads to the formation of an efficient ternary complex. Thus, this implies a conformational rearrangement occurring during the catalytic turnover of the E268A mutant. Its nondetection in the binary complex E268A mutant−NADP remains to be explained and leaves open the question of the nature of the amino acid with a pK_{app} of 7.6.

In that regard, the pH−rate profiles for the acylation step in wild type and in E268A mutant were recently determined. They showed bisigmoidal and monosigmoidal dependencies with pK_{app} of 6.2 and 7.5, and with pK_{app} of 6.2, respectively (Marchal et al., unpublished results). Therefore, Glu-268 is likely the amino acid with a pK_{app} of 7.6 and is not involved in the stabilization of the thiolate form. The major role of Glu-268 would be to activate the water molecule that attacks the thioacyl intermediate (Marchal et al., unpublished results). The fact that the pK_{app} of Cys-302 was 6.78 in the presence of saturating concentration of NADPH compared to 6.1 in the presence of NADP supports a minor role of the positive charge of the nicotinamide ring in the pK_a decrease of Cys-302. Thus, structural factors, which remain to be characterized, should be revealed during the conformational rearrangement to stabilize the thiolate form of Cys-302.

The absence of detectable conformational rearrangement in the binary complex C302A mutant-NADP also raised the question of the role of the thiol group in favoring the rearrangement in the wild type. The addition of G3P to the C302A mutant complexed with NADP strongly accelerates the rate of the conformational rearrangement as proved by the value of the fluorescence quenching, which was showed to be similar to that of the holo wild-type binary complex. Therefore, it can be concluded that formation of the covalent bond between the thiolate of Cys-302 and the aldehydic function of the substrate in the ternary complex is not a prerequisite for an efficient conformational rearrangement.

Four X-ray structures of ALDHs are available so far which have been determined either in the presence or the absence of cofactors. As already mentioned in the introduction section, inspection of the structures of all four ALDHs does not give obvious indications on the nature of the structural and molecular factors which could explain the observed low pK_{app} and high chemical reactivity of Cys-302 in the holo-form of GAPN of *S. mutans*. In all the reported structures the distance between the side chains of Cys-302 and Glu-268 are higher than 6 Å. This distance is not compatible with our biochemical studies which show a conformational rearrangement occurring within the active site during the cofactor binding which not only renders Cys-302 more accessible and more reactive at physiological pH but brings Cys-302 and a residue, which is likely Glu-268, closer to each other (less than 4 Å). This rearrangement also depends on the protonation of an amino acid with a pK_{app} of 5.7 whose nature remains to be determined. The rearrangement should consist of at least reorientation of both the side chains of Cys-302 and Glu-268 and likely repositioning of the nicotinamide ring of the cofactor which permits not only the chemical activation of Cys-302 but also the formation of an efficient ternary complex. These conclusions are not in contradiction with recent structural data and modeling of the transition state complex on different ALDHs which suggest repositioning of the nicotinamide ring and (or) of the side chains of Cys-302 and Glu-268 during the catalytic event (*10*−*13*). Thus, it is likely that the conformation of the active site of the holo structures described so far does not exactly represent the biologically active form. The knowledge of the X-ray structure of a ternary complex of GAPN from of *S. mutans* which is currently under study (Cobessi et al., unpublished results) should shed more light on this issue.

ACKNOWLEDGMENT

Thanks are due to D. A. Boyd, D. G. Cvitkovitch, and I. R. Hamilton for providing *gapN* plasmid construction and to H. O. Spivey and S. Rahuel-Clermont for helpful discussions. We are very grateful to N. Zorn and A. Van Dorsselaer for determining the molecular weights of wild-type and mutant GAPNs. We also thank the Service Commun de Biophysicochimie of University Henri Poincaré, Nancy I, for giving us the possibility to realize molecular modeling and E. Habermacher, S. Boutserin, and S. Azza for their very efficient technical help.

REFERENCES

1. Crow, V. L., and Wittenberger, C. L. (1979) *J. Biol. Chem*. *254*, 1134−1142.
2. Lindahl, R. (1992) *Crit. Rev. Biochem. Mol. Biol*. *27*, 283−335.
3. Perozich, J., Nicholas, H., Wang, B. C., Lindahl, R., and Hempel, J. (1999) *Protein Sci. 8*, 137−146.
4. Feldman, R. I., and Weiner, H. (1972) *J. Biol. Chem*. *247*, 267−272.
5. Dunn, M. F., and Buckley, P. D. (1985) *Prog. Clin. Biol. Res*. *174*, 15−27.
6. Abriola, D. P., Mackerell, A. D., and Pietruszko, R. (1990) *Biochem. J. 266*, 179−187.
7. Blatter, E. E., Abriola, D. P., and Pietruzsko, R. (1992) *Biochem. J. 282*, 353−360.
8. Farres, J., Wang, T. T., Cunningham, S. J., and Weiner, H. (1995) *Biochemistry 34*, 2592−2598.
9. Hempel, J., Nicholas, H., and Lindahl, R. (1993) *Protein Sci*. *2*, 1890−1900.
10. Steinmetz, C. G., Xie, P., Weiner, H., and Hurley, T. D. (1997) *Structure 5*, 701−711.
11. Liu, Z. J., Sun, Y. J., Rose, J., Chung, Y. J., Hsiao, C. D., Chang, W. R., Kuo, I., Perozich, J., Lindahl, R., Hempel, J., and Wang, B. C. (1997) *Nat. Struct. Biol*. *4*, 317−326.
12. Johansson, K., El-Ahmad, M., Ramaswamy, S., Hjelmqvist, L., Jörnvall, H., and Eklund, H. (1998) *Protein Sci*. *7*, 2106−2117.
13. Moore, S. A., Baker, H. M., Blythe, T. J., Kitson, K. E., Kitson, T. M., and Backer, E. N. (1998) *Structure 6*, 1541−1551.
14. Boyd, D. A., Cvitkovitch, D. G., and Hamilton, I. R. (1995) *J. Bacteriol*. *177*, 2622−2627.
15. Kunkel, T. A., Bebenek, K., and McClary, J. (1991) *Methods Enzymol*. *204*, 125−139.
16. Laemmli, U. K. (1970) *Nature 227*, 680−685.
17. Scopes, R. K. (1974) *Anal. Biochem*. *59*, 277−282.
18. Segel, H. I. (1968) in *Enzyme kinetics. Behavior and analysis of rapid equilibrium and steady-state enzyme system*, 3rd ed., John Wiley & Sons, Inc., New York.
19. Corbier, C., Mougin, A., Mely, Y., Adolph, H. W., Zeppezauer, M., Gerard, D., Wonacott, A., and Branlant, G. (1990) *Biochimie 72*, 545−554.
20. Stockell, A. (1959) *J. Biol. Chem. 234*, 1286−1292.
21. Wang, X., and Weiner, H. (1995) *Biochemistry 34*, 237−243.
22. Vedadi, M., and Meighen, E. (1997) *Eur. J. Biochem*. *246*, 698−704.
23. Talfournier, F., Colloc'h, N., Mornon, J. P., and Branlant, G. (1998) *Eur. J. Biochem*. *252*, 447−457.

BI990453K